The Journal of Experimental Biology 214, 2631-2640

doi:10.1242/jeb.049544

RESEARCH ARTICLE

In vivo strains in the femur of the Virginia opossum (*Didelphis virginiana*) during terrestrial locomotion: testing hypotheses of evolutionary shifts in mammalian bone loading and design

Michael T. Butcher[1], Bartholomew J. White[1], Nathan B. Hudzik[1], W. Casey Gosnell[2], John H. A. Parrish[2,3] and Richard W. Blob[2,*]

[1]Department of Biological Sciences, Youngstown State University, Youngstown, OH 44555, USA, [2]Department of Biological Sciences, Clemson University, Clemson, SC 29634, USA and [3]Research Services, Clemson University, Clemson, SC 29634, USA

*Author for correspondence (rblob@clemson.edu)

Accepted 10 March 2011

SUMMARY

Terrestrial locomotion can impose substantial loads on vertebrate limbs. Previous studies have shown that limb bones from cursorial species of eutherian mammals experience high bending loads with minimal torsion, whereas the limb bones of non-avian reptiles (and amphibians) exhibit considerable torsion in addition to bending. It has been hypothesized that these differences in loading regime are related to the difference in limb posture between upright mammals and sprawling reptiles, and that the loading patterns observed in non-avian reptiles may be ancestral for tetrapod vertebrates. To evaluate whether non-cursorial mammals show loading patterns more similar to those of sprawling lineages, we measured *in vivo* strains in the femur during terrestrial locomotion of the Virginia opossum (*Didelphis virginiana*), a marsupial that uses more crouched limb posture than most mammals from which bone strains have been recorded, and which belongs to a clade phylogenetically between reptiles and the eutherian mammals studied previously. The presence of substantial torsion in the femur of opossums, similar to non-avian reptiles, would suggest that this loading regime likely reflects an ancestral condition for tetrapod limb bone design. Strain recordings indicate the presence of both bending and appreciable torsion (shear strain: 419.1±212.8 με) in the opossum femur, with planar strain analyses showing neutral axis orientations that placed the lateral aspect of the femur in tension at the time of peak strains. Such mediolateral bending was unexpected for a mammal running with near-parasagittal limb kinematics. Shear strains were similar in magnitude to peak compressive axial strains, with opossum femora experiencing similar bending loads but higher levels of torsion compared with most previously studied mammals. Analyses of peak femoral strains led to estimated safety factor ranges of 5.1–7.2 in bending and 5.5–7.3 in torsion, somewhat higher than typical mammalian values for bending, but approaching typical reptilian values for shear. Loading patterns of opossum limb bones therefore appear intermediate in some respects between those of eutherian mammals and non-avian reptiles, providing further support for hypotheses that high torsion and elevated limb bone safety factors may represent persistent ancestral conditions in the evolution of tetrapod limb bone loading and design.

Supplementary material available online at http://jeb.biologists.org/cgi/content/full/214/15/2631/DC1

Key words: locomotion, biomechanics, bone strain, opossum, safety factor.

INTRODUCTION

Among terrestrial tetrapods, locomotion is often a critical but demanding behavior that can place high demands on many body systems. The skeletal system may be especially taxed during locomotion over land as, in many species, running is thought to impose the highest loads that limb bones experience (Biewener, 1990; Biewener, 1993). But although the significance of locomotion to limb bone loading is broadly appreciated, comparative data on locomotor loading across a broad range of tetrapod lineages, limb designs and locomotor habits have only recently started to be assembled.

Data on limb bone loading have been collected in numerous studies of mammals and ground-dwelling birds that use parasagittal limb kinematics (Rubin and Lanyon, 1982; Biewener et al., 1986; Biewener et al., 1988; Carrano, 1998; Demes et al., 2001; Lieberman et al., 2004; Main and Biewener, 2004; Main and Biewener, 2007), but recent examinations of limb bone loading in reptilian (Blob and Biewener, 1999; Blob and Biewener, 2001; Butcher and Blob, 2008; Butcher et al., 2008; Sheffield et al., 2011) and amphibian (Sheffield and Blob, 2011) lineages that employ sprawling limb posture have expanded perspectives on the diversity of bone loading patterns and mechanics among tetrapod clades. In birds and mammals, limb bones are typically loaded with high magnitudes of bending and axial compression (Biewener, 1990; Biewener, 1991), although significant torsion has been found in the hindlimbs of some running birds (Carrano, 1998; Main and Biewener, 2007) and one species of small mammal [laboratory rat (Keller and Spengler, 1989)]. Avian and mammalian limb bones also exhibit generally similar mechanical properties and resistance to failure (Biewener, 1982; Erickson et al., 2002) that, when compared with *in vivo* loads, lead to safety factors in the range of 2 to 4 (Alexander, 1981; Biewener, 1993). In contrast, taxa that use more sprawling limb postures, including iguanas and alligators (Blob and Biewener, 1999; Blob and Biewener, 2001), turtles (Butcher and Blob, 2008; Butcher et al.,

2008), tegus (Sheffield et al., 2011) and salamanders (Sheffield and Blob, 2011), tend to show moderate levels of bending and axial compression with more prominent limb bone torsion than quadrupedal mammals, but also higher limb bone safety factors than birds or mammals.

It is possible that the strong differences in limb bone loading patterns in amphibians and non-avian reptiles *versus* birds and mammals could reflect adaptations of these lineages to differing locomotor demands. For example, the high safety factors of amphibians and non-avian reptiles might help to accommodate lower rates of bone remodeling (de Ricqlès, 1975; de Ricqlès et al., 1991) or higher load variability (Lowell, 1985) than typically occur in birds and mammals (Blob and Biewener, 1999; Blob and Biewener, 2001). Yet, the similarities observed in many aspects of limb bone loading among the growing number of amphibian and non-avian reptile lineages examined supports the possibility that loading patterns observed in amphibians and non-avian reptiles may represent ancestral conditions from which birds and mammals independently diverged (Sheffield et al., 2011). This latter possibility, however, leaves open the question of when divergence in bone loading patterns took place in the evolutionary history of these lineages. Studies of locomotor ground reaction forces (GRFs) across diverse amphibian, reptilian, avian and mammalian lineages have shown only limited differences in GRF orientation across species, indicating that differences in bone loading across taxa relate predominantly to differences in limb posture and kinematics (Jayes and Alexander, 1980; Biewener, 1983a; Biewener, 1983b; Biewener et al., 1983; Biewener, 1989; Blob and Biewener, 2001; Butcher and Blob, 2008). Thus, to understand how limb bone loading patterns changed through the course of amniote evolution, data on limb bone loading from species using kinematics that differ from those that have received the most attention (sprawling reptiles and upright, cursorial mammals) could provide important insights.

To help evaluate whether non-cursorial mammals show loading patterns more similar to those of sprawling lineages, we measured *in vivo* terrestrial locomotor strains in the femur of the Virginia opossum (*Didelphis virginiana*). We also compared strain magnitudes with bone mechanical property data from didelphids to calculate limb bone safety factors. Opossums use a more crouched limb posture (Jenkins, 1971a) than the cursorial mammals (e.g. dogs, goats and horses) from which most limb bone strain data have been collected, providing an opportunity to evaluate the impact of this limb kinematic pattern on limb bone loading. *Didelphis virginiana* also uses a different locomotor gait than cursorial mammals, constrained to running only at a trot rather than transitioning to a gallop to achieve higher speeds (Peters et al., 1984; White, 1990; Reilly and White, 2003). Moreover, as a marsupial, *D. virginiana* belongs to a clade phylogenetically between non-avian reptiles and the eutherian mammals (Bishop and Friday, 1987; Kirsh and Mayer, 1998; Meyer and Zardoya, 2003) that have been the primary focus of most studies of limb bone loading. Didelphids are commonly viewed as the most basal marsupial lineage (Asher et al., 2004; Beck, 2008), though the most basal members of the clade [e.g. *Glironia*, *Caluromys* and *Caluromysiops* (Voss and Jansa, 2009)] exhibit arboreal habits and specializations (Nowak, 1991). However, although retaining features such as grasping feet and a prehensile tail, *D. virginiana* and the other opossum genera to which it is most closely related [*Philander* and *Lutreolina* (Voss and Jansa, 2009)] are primarily terrestrial rather than arboreal (Jenkins, 1971a; Nowak, 1991; Delciellos and Vieira, 2006; Delciellos and Vieira, 2009). As a result of this convergence back to terrestrial habits, *D. virginiana* may not represent the specific 'intermediate' between the locomotor patterns of non-avian reptiles and cursorial mammals, but they provide a functional analog of such an intermediate that is appropriate for comparison to other lineages in which limb bone loading has been evaluated. In this context, the presence of substantial torsion in the femur of opossums during locomotion, unlike cursorial mammals but similar to non-avian reptiles, might suggest the persistence of an ancestral condition of tetrapod limb bone function into the mammalian clade. Our study of limb bone strains in the opossum will therefore, allow us to further test hypotheses that lower limb bone loads, high safety factors and prominent limb bone torsion are ancestral traits characteristic of lineages that do not hold their limbs upright in locomotion.

MATERIALS AND METHODS

Animals

Strain data were collected from five Virginia opossums, *Didelphis virginiana* (Kerr 1927) (four females and one male, 1.6–3.9 kg body mass). Opossums were captured locally (Pickens and Anderson Counties, SC, USA) using live traps (Havahart EasySet, 32×12×14 inches; Forestry Suppliers, Jackson, MS, USA). Animals were housed in medium-sized primate enclosures equipped with fresh water and litter pans, fed dog or cat food daily and exposed to 12 h:12 h light:dark cycles. Prior to experiments, opossums were given multiple training sessions involving 10–15 min bouts of exercise at moderate-to-high speeds on a motorized treadmill (model DC5; Jog A Dog®, Ottawa Lake, MI, USA), exposing them to the experimental conditions.

Surgical procedures

Strain gauges were attached surgically to the right femur of each animal using aseptic technique and following published methods (Biewener, 1992; Blob and Biewener, 1999; Butcher et al., 2008). All surgical and experimental procedures followed protocols approved by the Clemson University IACUC (AUP ARC2007-030 and 2009-059). Initial intramuscular doses of 2 mg kg^{-1} carprofen and 20 mg kg^{-1} ketamine were injected to induce analgesia and anesthesia, respectively, along with an intramuscular antibiotic injection (20 mg kg^{-1} Baytril). Opossums were then masked with isoflurane gas while rested on a heating pad, intubated for general anesthesia (isoflurane) and positioned to allow sterile surgical access to the lateral aspect of the right hindlimb.

To expose strain gauge attachment sites, a longitudinal incision was made through the skin on the anterolateral aspect of the thigh at mid-shaft. Muscles surrounding the femur were separated along the fascial plane between the vastus lateralis and biceps femoris, which were retracted to gain access to the femur. Gauges were attached at mid-shaft *via* this incision. At the site where gauges were to be attached, a 'window' of periosteum was removed to expose the bone cortex. Bone surfaces were scraped with a periosteal elevator, swabbed clean with ether using a cotton-tipped applicator and allowed to dry for several seconds. Gauges were then attached using a self-catalyzing cyanoacrylate adhesive (Duro™ Superglue; Henkel Loctite Corp., Avon, OH, USA).

Single element (SE) and rosette (ROS) strain gauges (types FLG-1-11 and FRA-1-11, respectively; Tokyo Sokki Kenkyujo, Tokyo, Japan) were attached to surfaces of the femur designated as anterior, lateral and posterior, following common conventions of anatomical orientation for mammals. Precise anatomical locations were determined from sections of the bones after the completion of the experiments (see below). One ROS gauge was used in each individual at the anterior location (individuals op4, op5 and op6). One SE gauge was attached to each of the other bone surfaces after

placement of the ROS (total of three gauges about the femur cross-section). The SE gauge and the central elements of the ROS gauge were aligned (within 5 deg) to the long axis of the femur. Once all gauges were in place, lead wires from the gauges (336 FTE, etched Teflon; Measurements Group, Raleigh, NC, USA) were passed subcutaneously though a small skin incision on the dorsolateral aspect of the hip (near the sacral vertebrae) and passed through a small hole in a Velcro® flap-patch sutured to the animal's skin, which provided protection for the wires during recovery. After all incisions were sutured closed, lead wires were soldered into a microconnector and solder connections were reinforced with epoxy. The microconnector then was secured (with slack) within the Velcro patch by fastening the flap cover.

In vivo strain data collection and data analysis

After 1–2 days of recovery, *in vivo* strain recordings were collected from opossums while the animals ran on the motorized treadmill used for locomotor training. Strain signals were conducted from the gauges to Vishay conditioning bridge amplifiers (model 2120B; Measurements Group) *via* a shielded cable. Raw voltage signals from strain gauges were sampled through an A/D converter (model PCI-6031E; National Instruments Corp., Austin, TX, USA) at 2000 Hz, saved to computer using data acquisition software written in LabVIEW™ (v.6.1; National Instruments) and calibrated to microstrain ($\mu\varepsilon$=strain$\times10^{-6}$). Trials consisted of short bouts of steady-speed trotting (0.84–1.9 m s^{-1}) with data sampled from 10–20 consecutive footfalls of the right hindlimb. In general, the speeds achieved by each opossum required considerable exertion and were close to the maximal speed that animals could sustain during trotting. Several minutes of rest were given between each locomotor trial.

To document locomotor behavior and footfall patterns during experiments, lateral and posterior views of strain trials were recorded with high-speed (100 Hz) video (Phantom V4.1; Vision Research Inc., Wayne, NJ, USA). Video data were synchronized with strain recordings using an LED visible in the video that simultaneously produced 1.5 V pulses visible in the strain records. Upon completion of strain recordings, animals were anesthetized (20 mg kg^{-1} intramuscular ketamine injection) and then killed by an overdose of pentobarbital sodium solution (Euthasol®, Delmarva Laboratories Inc., Midlothian, VA, USA; 200 mg kg^{-1} intracardiac injection) and frozen for later dissection, verification of strain gauge placement and measurement of limb bone mechanical properties.

Standard conventions for analysis and interpretation of strain data were employed, following our studies of limb bone loading in other species (Blob and Biewener, 1999; Butcher et al., 2008; Sheffield et al., 2011). Briefly, the magnitudes of peak axial strains (aligned with the long axis of the femur) were determined from each gauge location for N=40–60 steps from each opossum (with up to 60 steps analyzed if this number of adequate footfalls were available for an individual). For each consecutive footfall, raw strains were zeroed during swing phase just before limb contact with the ground (defined as 'toe down' from the video records), with tensile strains recorded as positive and compressive strains as negative. The distribution of tensile and compressive strains on the femoral cortex then was used to evaluate the loading regime to which the bone was exposed during locomotion. For instance, for the nearly circular cross-section of the opossum femur, equal magnitudes of tensile and compressive strain on opposite sides of the cortex would indicate pure bending, whereas unequal magnitudes of tension and compression on opposite cortices would indicate a combination of axial and bending loads. Magnitudes and orientations of peak principal strains (i.e. maximum and minimum strains at each site, regardless of alignment with the femoral long axis), as well as shear strain magnitudes, were calculated from ROS data following published methods (Carter, 1978; Dally and Riley, 1978; Biewener and Dial, 1995), allowing evaluation of torsional loading in opossum femora. Defining the long axis of the femur as 0 deg, pure torsional loads would show principal strain orientations (deviations from the bone long axis) of 45 or –45 deg depending on whether the femur was twisted in a clockwise or counterclockwise direction, respectively.

Following dissections of the hindlimb musculature of each opossum, instrumented femora were excised, swabbed clean of soft tissue and embedded in fiberglass resin. Transverse sections were cut from each embedded femur through the mid-shaft gauge locations, and one cross-section from each bone was then photographed using a digital camera mounted on a dissecting microscope. Microsoft PowerPoint was used to trace endosteal and periosteal outlines of the cross-sections from the photographs, mark locations of the three gauges on the bone perimeter and save cross-sectional tracings as JPEG files. Each bone's geometric data were then input along with strain data from the three femoral gauge locations into analysis macros for the public domain software NIH Image for Macintosh, allowing calculation of the location of the neutral axis (NA) of bending and the planar distribution of longitudinal strains through femoral cross sections (Lieberman et al., 2003; Lieberman et al., 2004). Planar strain analyses were conducted on a subset of data (N=37 steps; two individuals), in order to calculate estimates of peak tensile and compressive strain that may have occurred at locations other than recording sites (Carter et al., 1981; Biewener and Dial, 1995). Calculated peak strains were then compared with measured peak strains to determine the proportional increase in strain between the recorded peaks and calculated peak magnitudes (Blob and Biewener, 1999; Butcher et al., 2008). Additionally, in a subset of these data (N=32; 16 steps per individual), planar strain distributions were calculated at five time points during a step (15, 30, 50, 70 and 85% of contact) (Butcher et al., 2008; Sheffield et al., 2011) to evaluate shifts in the location and orientation of the NA throughout the step.

Mechanical properties and safety factors

Because data for femoral mechanical properties in bending have been published for the closely related opossum species *D. marsupialis* (Erickson et al., 2002), we focused the use of our specimens on the measurement of femoral mechanical properties in torsion. Yield strains were evaluated in torsion (model 8874 biaxial testing machine with 25 kN load cell; Instron, Norwood, MA, USA) for whole bone specimens (N=7 femora) that had not been instrumented during *in vivo* strain trials. Procedures generally followed those described previously for turtle (Butcher and Blob, 2008; Butcher et al., 2008), frog (Wilson et al., 2009) and lizard (Sheffield et al., 2011) femora. Briefly, femora were extracted from thawed opossum specimens, and muscle and periosteal tissue were cleaned away with moistened cotton swabs. Bones were suspended in machined aluminum wells into which dental cement was poured to embed ~15 mm of the end of each bone. Once the cement hardened, ROS gauges were attached to the anterior and posterior surface of each bone at mid-shaft, and the embedded ends were fitted into mounting brackets in the testing jig. Gauge lead wires were soldered to a microconnector that was plugged into a shielded cable to convey raw strain signals to the Vishay amplifiers used during *in vivo* strain recordings. Amplified strain signals were sampled through an A/D converter in LabVIEW at 500 Hz, and calibrated as detailed for *in vivo* recordings. Bones were twisted to

failure at 3 deg s^{-1} (Furman and Saha, 2000), with tests performed to simulate *in vivo* medial (i.e. inward) rotation.

Yield point was identified from linear plots of applied twisting moment (torque) *versus* maximum shear strain as the first point where measured strain magnitude deviated from the magnitude expected based on the initial linear slope of the curve by 200 με (Currey, 1990). Strain-based safety factors in shear for the femur of *D. virginiana* were calculated using two slightly different approaches. In the first, safety factor was calculated as the ratio of the mean yield strain across all of our mechanical property tests and the mean of the highest strain magnitude calculated for each individual (corrected for proportional value of strain increase determined from planar strain analyses). In the second, a separate safety factor was calculated for each opossum as the ratio of the mean yield strain for the species and peak locomotor strain for each individual (corrected based on planar strain analyses); the safety factor values were then averaged to characterize the opossum femur. This second method was executed as described so that parallel approaches to calculations could be performed between shear and bending [for which mechanical property values were taken from a different study (Erickson et al., 2002)]. Application of the planar strain correction factor to shear strains requires the assumption that shear strains increase in proportion to normal strains around a bone cortex. Though an oversimplification, this assumption prevents underestimation of shear strains that would artificially inflate safety factor estimates. In addition to torsional safety factors, safety factors in bending also were calculated using the same two approaches. Peak functional strain values were evaluated by multiplying mean values of measured peak compressive strains by the proportional increase in strain determined from planar strain analyses. Compressive yield strain in bending was calculated from previously published (Erickson et al., 2002) tensile yield strains in bending for *D. marsupialis*, with the assumption that tensile yield strains are typically only 75% of compressive yield strains in bending (Biewener, 1993).

RESULTS

Locomotor strain patterns and magnitudes

Generalizations about femoral strains in running opossums were made based on the most common strain patterns observed for each recording site. Peak strain magnitudes were moderately variable among the five instrumented opossums (coefficients of variation averaged 24.0% across ROS recordings from the anterior gauge location). Also, because of minor differences in gauge placement, recordings from sites near the NA (as determined by planar strain analyses) showed some variation among individuals as to whether peak strains were tensile or compressive, and in the magnitude of recorded strains (Fig. 1A,B). However, patterns of tensile and compressive strain at each recording location were largely consistent between steps for each individual, allowing typical loading patterns to be evaluated.

Axial strains from the anterior location were consistently compressive throughout the step across all individuals (Fig. 1). Axial strains from the lateral and posterior locations showed some shifts between tension and compression during the step, though the primary peaks were tensile at the lateral location and either tensile or compressive at the posterior location depending on the individual (Fig. 1). Axial strain peaks from the lateral location occurred earlier than axial, principal and shear peaks from the anterior location, which occurred near mid-stance (Fig. 1). Timing of axial strain peaks at the posterior location was variable, occurring later in the step in individuals for which the primary peak was compressive (e.g. 80.9±6.2% contact in op4, Fig. 1A), but earlier in the step (in synchrony with peaks from the lateral location) in individuals for which the posterior location showed greater fluctuation between tension and compression during the step (e.g. individual op5, Fig. 1B). These strain distributions and the relative magnitudes of tension and compression around the cortex indicate that the opossum femur is loaded in a combination of axial compression and bending. Compressive strains from the anterior location were generally higher in magnitude than tensile and compressive strains at the other two sites, and this pattern of strain was generally consistent across individuals. Posterior strain records in a single individual (op4), however, showed the highest absolute magnitudes of compressive strain across the opossums we tested, causing mean (pooled) strains to have the highest value at this location (–713.4±695.3 με; Table 1, supplementary material Table S1).

Principal (and shear) strain recordings typically showed two peaks (Fig. 1A). In three individuals, axial peaks from the anterior location occurred between the peaks of principal and shear strains from the same location. Recorded strain patterns for individual op5 varied from the typical pattern by showing one peak per step for both principal and shear strains (Fig. 1B). Principal and shear strain data indicate that, in addition to bending and axial compression, opossum femora experience significant torsion. Mean orientations of peak principal tensile strain (ϕ_t) on the anterior surface of the femur deviated from the long axis of the bone, with values averaging 37.1±8.2 deg (Table 1, Fig. 1), approaching the 45 deg value expected for pure torsional loading. Based on conventions for gauge configurations in our experiments, positive mean values for ϕ_t indicated medial rotation of the femur during the step. Peak shear strains were appreciable, averaging 419.1±212.8 με (Table 1) across individuals, a value comparable to those recorded from rat femora (Keller and Spengler, 1989), but high for the limb bones of upright mammals [e.g. goats (Main and Biewener, 2004)]. For one individual (op4), mean shear strain on the anterior surface was 676.0±209.9 με, similar to values reported for the same surface of the tibia and the homologous 'dorsal' surface of the femur in alligators during running (Blob and Biewener, 1999). Femoral shear strains in opossum generally exceeded mean peak principal strain measurements (compressive) by approximately 30% (Table 1, Fig. 1).

Analyses of planar strain distribution and NA orientation

Planar strain analyses were conducted for two individuals (op4 and op5) for which we successfully recorded from all three gauge sites, including the anterior ROS gauge. Though some variation in absolute NA orientation and location about the femur cross-section was evident, similar patterns emerged across the trials analyzed, particularly through the first half of stance phase (i.e. the first three time points examined). At the beginning of the step, the NA was typically aligned near the anatomical anteroposterior (AP) axis, but shifted lateral from the cross-sectional centroid (Figs 2, 3). As strain magnitudes increased through the step (30% contact), the NA consistently shifted more laterally and became more closely aligned with the anatomical AP axis (Figs 2, 3), placing the lateral aspect of the cortex in net tension. In addition, the displacement of the NA from the centroid and the extent of compressive strains across the femoral cross-section confirm loading in axial compression, in addition to bending and torsion, for opossum femora. By mid-stance, the NA shifted further laterally to place most of the femoral cross-section in compression, although peak magnitudes of tensile and compressive strain differed between individuals. Through the last half of the step, the orientation of the NA remained close to the anatomical AP axis (Fig. 3). In one individual (op5), planar analyses indicated a shift in strain distributions late in the step, such that the lateral and posterior aspects of the femur were placed in compression and the medial and anterior aspects were placed in tension (Fig. 3B).

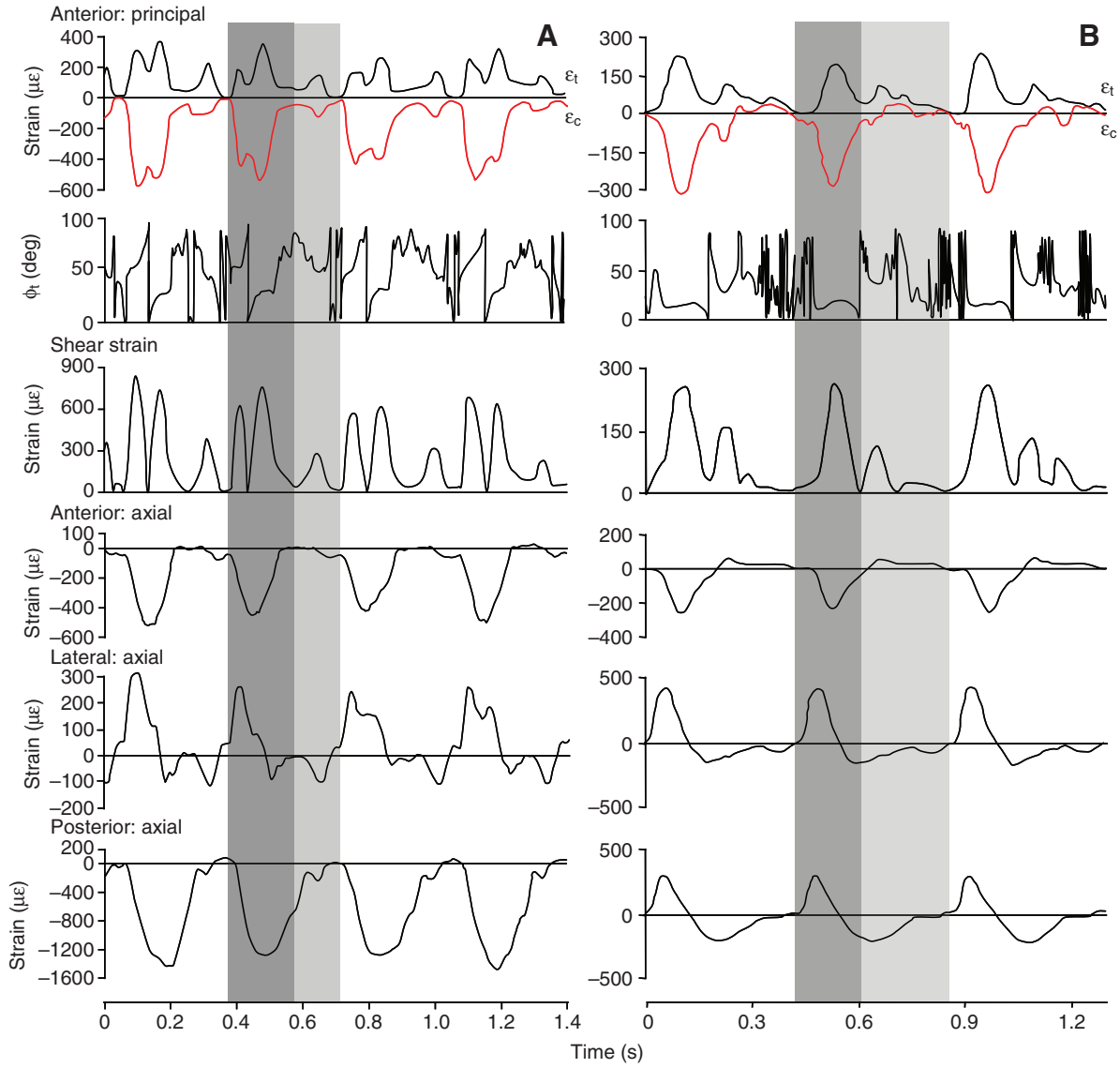

Fig. 1. Representative strain recordings (simultaneous) from three gauge locations on the opossum femur during three to four consecutive running steps (at 1.2 m s^{-1}) for two individuals, op4 (A) and op5 (B), that show pattern variations discussed in the text. Principal strains, angle of principal tensile strains from the femoral long axis (ϕ_t) and shear strains from ROS gauge recordings on the anterior surface are shown, as well as axial strains from anterior, lateral and posterior locations. Note that strain scales differ among panels to facilitate presentation. Dark gray shading marks the stance phase (contact) for a single step at all gauge locations; light gray shading marks the swing phase of a stride. Top trace: ε_t and ε_c denote tensile (black line) and compressive (red line) principal strains, respectively.

However, strain magnitudes were well below peak at the 70 and 85% time points in the step, and the plane of bone bending in this individual remained close to the anatomical AP axis through the last half of the step (Figs 2, 3).

Planar strain data indicate that peak tensile strains occur on the lateral aspect of the femur in opossums and peak compressive strains occur on the medial surface, rather than at the precise locations from which strains were recorded in the test animals. Based on the

Table 1. Peak axial (ε_{axial}), principal tensile (ε_t), principal compressive (ε_c) and shear strains recorded from the Virginia opossum (*Didelphis virginiana*) femur during locomotion

Gauge location	ε_{axial} (με)	ε_t (με)	ε_c (με)	ϕ_t (deg)	Shear (με)
Anterior	–379.4±248.9 (224, 5)	217.8±112.7 (152, 3)	–317.5±138.6 (152, 3)	37.1±8.2 (152, 3)	419.1±212.8 (152, 3)
Lateral	199.5±114.2 (141, 3)				
Posterior	–713.4±695.3 (103, 3)				

Values are means ± s.d. across all individuals; the number of steps analyzed and the number of individuals tested, respectively, are in parentheses.
Angles of principal tensile strains to the long axis of the bone (ϕ_t) are also reported.
Positive angles for ϕ_t indicate inward (medial) rotation for all gauge locations.

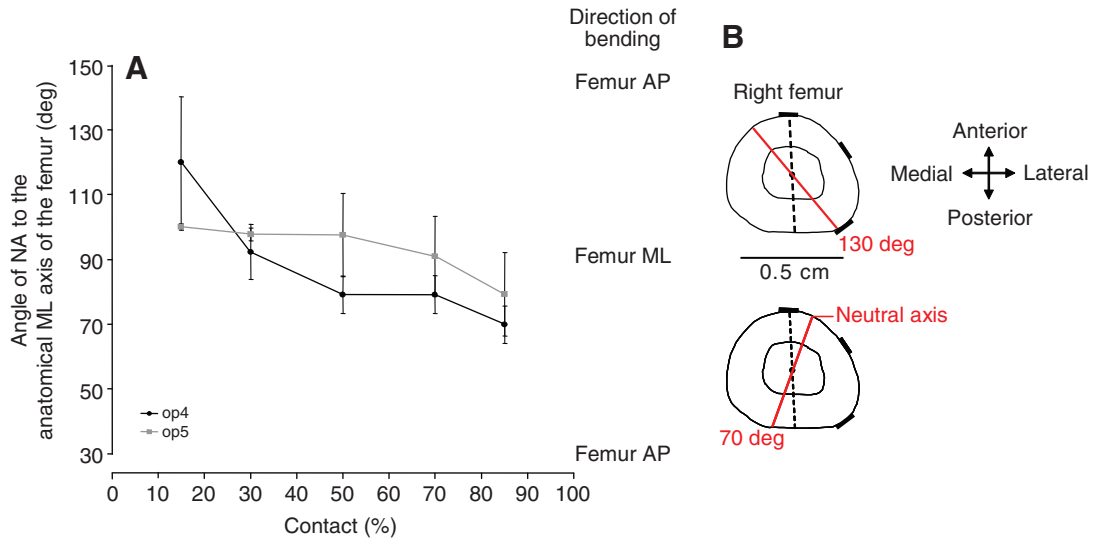

Fig. 2. (A) Shifts in the orientation of the neutral axis (NA) of femoral bending at five time increments (% of contact) through the duration of the step for two individual opossums. Each data point represents the angle of the NA to the anatomical mediolateral (ML) axis of the femur averaged over *N*=16 steps. The direction of bending indicated by these angular values is indicated by the scale to the right of the panel, with respect to the anatomical axes of the bone as described in the text, not in an absolute frame reference. AP, bending about an NA running from the anatomical medial to lateral cortex; ML, bending about an NA running from the anatomical anterior to posterior cortex. (B) Schematic cross-sections of the femur illustrating NA orientation and shift. Strain gauge locations are indicated by the black bars around the cortex of the cross-section. Solid red lines show the NA with an orientation of 130 deg (top) or 70 deg (bottom) relative to the anatomical ML axis; vertical dashed lines indicate the anatomical AP axis.

distribution of planar strain contours (Fig. 3), actual peak strains in the opossum femur are likely higher than those recorded, averaging 2.53±0.35 times higher (mean ± s.d.) across trials in which planar strain distributions were calculated (*N*=37 steps).

Bone mechanical properties and safety factors

Prior to calculating safety factors for the opossum femur, peak recorded functional strains (bending and shear) were multiplied by 2.53 to reflect the results of planar strain analyses. Because planar strain analyses indicated much higher compressive strains than tensile strains for opossum femora, bending safety factors were calculated using peak compressive strains (Sheffield et al., 2011). Assuming that tensile yield strains are typically only 75% of compressive yield strains in bending (Biewener, 1993), a value of –11611.3 με (Table 2) was calculated for the compressive yield strain of opossum femora based on tensile yield strain in bending reported for the femur of *D. marsupialis* [9289 με (Erickson et al., 2002)]. Based on the highest (calculated) strains determined across individuals, a mean value of –2272.3 με and a maximum value of –5069.1 με for peak functional strain were calculated. The ratio of bending yield strain to mean peak strain generated a safety factor estimate of 5.1, whereas our second method for calculating safety factors (based on the mean of safety factor values calculated for each individual) generated an estimate of 7.2 (Table 2, supplementary material Table S2).

Each bone failed catastrophically in torsion, with yield and fracture occurring nearly simultaneously. Yield strains in torsion were moderately higher for opossum femora (10815.7±1227.1 με, *N*=7; Table 2) than values previously reported for other species that use their limbs for terrestrial locomotion [8000–10,000 με (Currey, 1984; Keller and Spengler, 1989; Butcher et al., 2008; Wilson et al., 2009)]. Prior to safety factor calculations, peak functional shear strains recorded from opossum femora during locomotor trials were also multiplied by 2.53 to reflect proportional increases in strain predicted by results of planar strain analyses. Safety factors in shear were fairly similar to estimates for bending, with only slightly higher values of 5.5 estimated using our first approach and 7.3 using our second approach (Table 2, supplementary material Table S2).

DISCUSSION

Loading regimes and magnitudes in opossum femora: correspondence with expectations, comparisons with other species and mechanical interpretations

Direct measurements of *in vivo* strains indicated that opossum femora are exposed to a combination of loading regimes including axial compression, bending and torsion. Strain recordings showed both tensile and compressive strains on the femoral cortex that support the presence of bending, with planar strain analyses showing substantial displacement of the NA from the cross-sectional centroid of the femur, indicating that axial compression is superimposed on bending (Table 1, Figs 1, 3). The combination of axial compression and bending is common across a diverse range of tetrapods in which limb bone loads have been evaluated (Biewener et al., 1983; Biewener et al., 1986; Blob and Biewener, 1999; Demes et al., 2001; Lieberman et al., 2004; Main and Biewener, 2004; Main and Biewener, 2007; Butcher et al., 2008; Sheffield and Blob, 2011; Sheffield et al., 2011). However, planar strain analyses also show that NA orientation aligns very closely with the anatomical AP axis of the opossum femur, such that the bone is exposed to predominantly mediolateral (ML) bending that places the lateral cortex in tension and the medial cortex in compression at the time of peak strain (Figs 2, 3). ML bending of the femur was unexpected for a terrestrial mammal with limb kinematics that, although potentially deviating slightly from strict parasagittal motion (Jenkins, 1971a), are much closer to parasagittal than those of sprawling amphibians and non-avian reptiles.

Evaluations of the orientation of *in vivo* limb bone bending from other species, with which our data from opossums can be compared, are surprisingly limited. Many initial studies of limb bone loading in mammals focused primarily on the anterior and posterior cortices

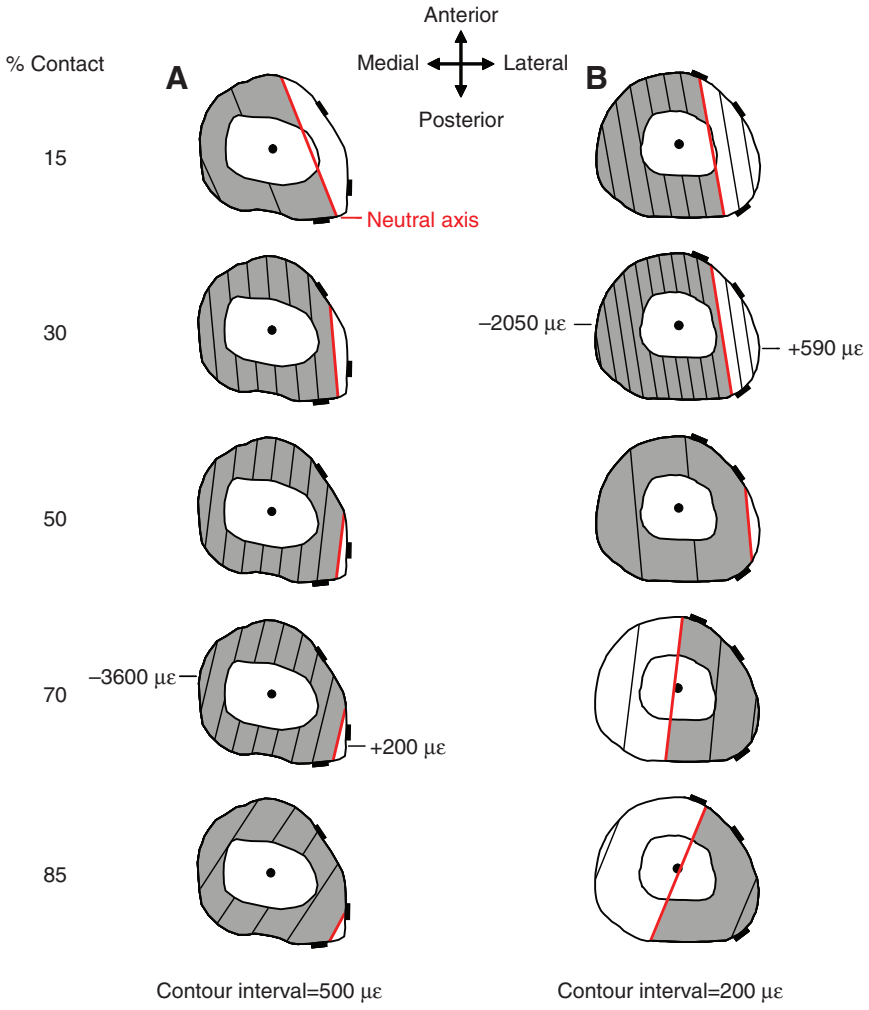

Fig. 3. Graphical comparisons of cross-sectional planar analyses of femoral strain distributions calculated for five time increments (% of contact) during representative steps for (A) op4 and (B) op5. Time increments (% of contact) correspond to those plotted in Fig. 2. The centroid of each section is indicated by the black dot. Thin lines indicate contours of strain magnitude, each representing 500 με for op4 and 200 με for op5. Peak strains calculated for these steps are labeled on the sections at either 70 or 30% depending on the individual. Compressive strains are shaded gray. The NA of bending (strain=0 με) is indicated by the red line (strain contour) separating compressive and tensile strains. Strain gauge locations are indicated by the black bars around the cortex of each cross-section. Anatomical directions are labeled to reflect the AP and ML axes illustrated in Fig. 2B.

of the skeletal elements (e.g. Rubin and Lanyon, 1982; Biewener, 1983a; Biewener et al., 1983; Biewener and Taylor, 1986), likely under a reasonable assumption that these locations would show the highest loads in species using parasagittal limb kinematics. However, recent studies that have measured strains across a greater range of limb bone locations in species including dogs (Szivek et al., 1992), horses (Gross et al., 1992), macaques (Demes et al., 2001) and sheep (Lieberman et al., 2004) have found expected patterns of near AP bending in hindlimb bones during locomotion at fast speeds, though bending orientation was more variable during slower locomotion. Strain data from the radius of goats (Main and Biewener, 2004) indicate ML bending that places the lateral surface in tension, much like our results for opossum femora, though this comparison is complicated by the presence of the ulna in the antebrachium. Thus, although not entirely unprecedented among mammalian limb bones, prominent ML limb bone bending may be a distinctive feature in either small mammals or species that use crouched limb posture. Examination of three-dimensional GRF data could provide insight into the mechanics that produce ML bending in opossum femora, particularly the relative contributions of the GRF and medial muscle groups (such as limb adductors) in generating femoral loading patterns. In addition, because small body size and crouched posture were typical of the earliest mammals (Jenkins and Parrington, 1976; Kemp, 1985; Kielan-Jawaroska and Gambarayan, 1994), ML limb bone bending may have an ancient history in the clade. An ancestral prominence of ML bending could help to explain curious

Table 2. Mechanical properties, estimated actual peak strains and safety factors for the femur in the Virginia opossum (*Didelphis virginiana*)

Mechanical properties			Mean peak strains		Single highest strains		'Mean' safety factors	
Yield strain bending (με)	Yield strain shear (με)	Proportional increase in strain	Calculated comp. bending (με)	Calculated shear (με)	Calculated comp. bending (με)	Calculated shear (με)	Femur bending	Femur shear
–11611.3*	10815.7±1227.1 (7)	2.53	–2272.3	1968.9	–5069.1	3483.1	5.1–7.2	5.5–7.3

Mechanical property values are means ± s.d.; the number of bones tested is in parentheses.
*Value estimated from tensile yield strain in *Didelphis marsupialis* (Erickson et al., 2002).
Peak strain estimates were calculated based on planar strain distributions; these provided a quantitative measure of the proportional increases in recorded strains (Table 1) used to determine estimated strains.
'Mean' safety factor calculations are described in the text.

evolutionary changes in the cross-sectional shape of hindlimb bones in the synapsid lineage, in which both the femur and tibia show changes from circular cross-sections among the earliest lineages (pelycosaurs), which used sprawling limb posture, to anteroposteriorly flattened cross-sections among basal therapsid lineages, in which posture first became more parasagittal (Romer, 1922; Blob, 2001). Such limb bone shapes would convey greater resistance to ML bending for a given amount of bone material among lineages in which the magnitude of limb bone bending may have increased in significance relative to torsion, and would not be expected if anteroposterior bending dominated in these groups.

The prominence of shear strains in opossum femora was also somewhat surprising. Our ROS data showed principal strain orientations approximately 37 deg from the long axis of the femur (Table 1), producing appreciable shear strains that suggest significant torsional loading. Recorded peak shear strain magnitudes were generally higher than peak principal strains, averaging greater than 400 με across all individuals (Table 1) and frequently exceeding 1000 με in one opossum, leading to a calculated estimate of peak shear strain just under 2000 με (Table 2). These shear magnitudes are somewhat lower than typically found for reptiles, for which calculated estimates of peak shear have ranged from 1200 to 2700 με across lizards, alligators and turtles (Blob and Biewener, 1999; Butcher et al., 2008; Sheffield et al., 2011). In comparison to other mammals, however, the shear strains found in opossums are larger than those typically found in cursorial mammals, but similar to values from rats, for which recorded shear magnitudes approaching 1000 με have been reported [though estimates of peak shear have not been calculated (Keller and Spengler, 1989)].

Among other lineages, prominent shear strains during terrestrial locomotion (>2000 με) have also been reported for the femora of running birds (Carrano, 1998; Main and Biewener, 2007). In birds, the near-horizontal orientation of the femur during stance has been cited as a primary factor contributing to torsional loading, based on force platform data indicating that the GRF imposes a substantial off-axis moment on the femur while it is in such a position (Carrano, 1998; Carrano and Biewener, 1999). Similar underlying mechanics may contribute to the elevated shear strains determined for the femora of rats and opossums, which, as small scansorial mammals (Lee and Cockburn, 1985), use a crouched limb posture while running that places the femur in an orientation close to horizontal for much of stance (Jenkins, 1971a; Biewener, 1983a; Biewener, 1989; Biewener, 1990; Keller and Spengler, 1989; Carrano, 1998). GRF data from running opossums would help to test this hypothesis. If true, however, it would suggest significant differences in the mechanism underlying limb bone torsion between mammals and non-avian reptiles. In alligators, limb retraction by the caudofemoral muscles causes medial (inward) rotation of the femur when strains are highest, opposing a GRF moment that would cause rotation in the opposite direction (Reilly et al., 2005). In contrast, with reduction of the caudofemoral muscles in the lineage leading to mammals and the advent of the gluteal muscles as major limb retractors (Romer, 1922; Kemp, 1982; Kemp, 1985), muscle-mediated long axis rotation of the femur should be minimized in mammals, leaving external moments from the GRF as a primary factor that could induce torsional loading. Even with such potential differences in underlying mechanisms between reptiles and mammals, however, torsion might still have been an ancestral feature of mammalian limb bone loading. As noted earlier, crouched limb posture that could expose the femur to torsional GRF moments is typical of small mammals (Biewener, 1983a; Biewener, 1989; Biewener, 1990), and fossil specimens show that the earliest mammals generally had body sizes much smaller than the opossums used in our study (Jenkins and Parrington, 1976; Kemp, 1982; Kemp, 1985; Hopson, 1991; Hopson, 1994). Still, it is currently unclear whether the torsion observed in laboratory rat femora (Keller and Spengler, 1989) represents an ancestral retention. As rodents, rats are nested deeply within the eutherian clade (Bishop and Friday, 1987; Kirsh and Mayer, 1998; Meyer and Zardoya, 2003) and strain data from lineages intervening between marsupials and rodents that would allow more detailed optimization of bone loading traits on mammalian phylogeny (e.g. xenarthrans) are not presently available.

Safety factors in opossum femora: comparisons and implications for the evolution of limb bone design in tetrapods

Measurements of *in vivo* strain and bone mechanical properties allowed the calculation of safety factor estimates for opossum femora in both bending and torsion (Table 2). Our two estimates of femoral safety factors in bending establish a likely range of 5.1–7.2, overlapping or somewhat lower than strain-based mean estimates previously reported for the femora of non-avian reptiles including alligators [6.3 (Blob and Biewener, 1999)], lizards [8.8–10.8 (Blob and Biewener, 1999; Sheffield et al., 2011)] and turtles [6.9 (Butcher et al., 2008)], but slightly higher (without overlap) than the values of 2–4 typically reported for avian and mammalian limb bones (Alexander, 1981; Lanyon and Rubin, 1985; Biewener, 1993). Differences in load magnitudes and bone mechanical properties contribute to variation in limb bone safety factors across these lineages. In comparison to other mammals, opossums show peak compressive bending strains of nearly –2300 με (calculated mean maximum; Table 2) that are similar to principal strain values recorded from the limb bones of a wide range of cursorial mammals running at similar relative speeds [–1600 to –3300 με (Rubin and Lanyon, 1982; Biewener et al., 1988; Biewener and Taylor, 1986; Davies et al., 1993; Main and Biewener, 2004)], and slightly lower than an estimated mean of approximately –2500 με (Biewener, 1993). However, failure strains of opossum femora in bending (–11,611.3 με; Table 2) are moderately higher than those for many mammals, for which typical values are less than –8000 με (Currey, 1984; Biewener, 1993; Erickson et al., 2002). In contrast, relative to non-avian reptiles (Blob and Biewener, 1999; Butcher et al., 2008; Sheffield et al., 2011), peak bending strains of opossum femora were moderately high, but resistance to bending was similar or slightly lower.

Our estimates of femoral safety factor in torsion for opossums ranged from 5.5 to 7.3 (Table 2). Comparable calculations of torsional safety factors for the limb bones of other mammals are lacking in the literature, but available data (Keller and Spengler, 1989) indicate an upper estimate (without correcting for planar strain distributions) of approximately 10 for the femora of rats. Though lower than this estimate for rats, our estimates for opossum femora show close proximity (or even overlap) with torsional safety factors previously calculated for the femora of non-avian reptiles, including iguana and tegu lizards [4.9 and 7.8, respectively (Blob and Biewener, 1999; Sheffield et al., 2011)], alligators [5.4 (Blob and Biewener, 1999)] and river cooter turtles [3.8 (Butcher et al., 2008)]. Opossums may achieve their torsional safety factors through a slightly different path than reptilians, as yield strains in shear for opossum femora (10,815.7±1227.1 με; Table 2) were higher than values previously measured from reptiles [9441 με for turtles and 9934 με for tegu lizards (Butcher et al., 2008; Sheffield et al., 2011)]. Yield strains in shear typically attributed to the limb bones of non-reptilian taxa [e.g. 8000 με (Currey, 1984)] are much lower, but rat

femora also appear to have higher resistance to torsion [yield strain: 10,018 με (Keller and Spengler, 1989)]. Although variation in mechanical properties has not typically been viewed as a major factor contributing to functional diversity in tetrapod limb bones (Biewener, 1982; Erickson et al., 2002), the presence of elevated resistance to torsion in the femora of species subject to high torsional loading could indicate correlated evolution of these aspects of limb bone design and function (Blob and Snelgrove, 2006). Alternatively, elevated mechanical resistance to limb bone torsion may be an ancestral trait in tetrapods from which lineages of large, upright mammals diverged.

Comparisons of limb bone mechanical properties and safety factors across taxa reinforce the significance of torsion as a loading regime in opossums, as *D. virginiana* appears to possess a margin of safety against torsional failure that is similar or only slightly higher than that for species in which torsion is the predominant loading regime. However, in contrast to the non-avian reptiles for which safety factors have been evaluated (Blob and Biewener, 1999; Butcher et al., 2008; Sheffield et al., 2011), femoral safety factors for bending and shear fall in a similar range for opossums, whereas in reptiles, safety factors for bending are typically higher than those for shear (Blob and Biewener, 1999). Thus, although the magnitudes of femoral safety factor for both of these loading regimes in opossums may be intermediate between values from reptiles and eutherian mammals, the greater similarity of safety factors for shear between opossums and reptiles suggests that this combination of intermediate safety factors results from an increase in the importance of bending that is superimposed on a retained importance of torsion. Morphological data from fossil 'mammal-like reptiles' (i.e. non-mammalian therapsids) also indicate an increase in the importance of bending as a loading regime for hindlimb bones through the evolutionary 'reptile-to-mammal' transition (Blob, 2001), matching the phylogenetic span through which limb posture shifted from sprawling to near parasagittal (Jenkins 1971b; Kemp, 1982; Kemp, 1985). Thus, although our data from opossums indicate a number of novel aspects in their hindlimb loading mechanics (e.g. mediolateral femoral bending), the influence of ancestral features of limb bone loading remains strong even in this basal mammalian species. Evaluation of when lower safety factors and further reduction in torsion began to characterize mammalian limb bone loading will require the collection of data from additional mammalian lineages, but such studies could help to determine the evolutionary timing of distinctions in limb bone loading patterns between non-avian reptiles and mammals.

ACKNOWLEDGEMENTS

We thank T. Maie for assistance with surgeries, dissections and experiments; D. Drevna and E. Roth for analyses of strain magnitude; T. Pruitt, T. Smith, T. Parker and D. Bailey for animal care at the Godley-Snell Research Center (Clemson); and two anonymous reviewers for comments on the manuscript draft. J. DesJardins, R. Rusly and E. Alvarez (Clemson Bioengineering) provided access to and assistance with mechanical testing equipment; C. Templeton and J. Scott (Clemson) assisted with mechanical property analyses; D. Lieberman (Harvard) provided software for planar analysis of limb bone strains; and S. Bennett (South Carolina Department of Natural Resources) coordinated permission for field collection of opossums (SCDNR Scientific Collecting Permits 54-2008 and 40-2009). Additional assistance with opossum collection was provided by J. Gosnell, J. Cummings, H. Schoenfuss, L. Schoenfuss and the Animal Control Departments of Pickens County and Pendleton, SC. Support by NSF (IOB-0517340) and the Clemson University and Youngstown State University Departments of Biological Sciences is gratefully acknowledged.

REFERENCES

Alexander, R. M. (1981). Factors of safety in the structure of animals. *Sci. Prog.* **67**, 109-130.

Asher, R. J., Swartz, I. and Sánchez-Villagra, M. R. (2004). First combined cladistic analysis of marsupial mammal interrelationships. *Mol. Phylogenet. Evol.* **33**, 240-250.

Beck, R. M. D. (2008). A dated phylogeny of marsupials using a molecular supermatrix and multiple fossil constraints. *J. Mammal.* **89**, 175-189.

Biewener, A. A. (1982). Bone strength in small mammals and bipedal birds: do safety factors change with body size? *J. Exp. Biol.* **98**, 289-301.

Biewener, A. A. (1983a). Locomotory stresses in the limb bones of two small mammals: the ground squirrel and chipmunk. *J. Exp. Biol.* **103**, 131-154.

Biewener, A. A. (1983b). Allometry of quadrupedal locomotion: the scaling of duty factor, bone curvature and limb orientation to body size. *J. Exp. Biol.* **105**, 147-171.

Biewener, A. A. (1989). Scaling body support in mammals: limb posture and muscle mechanics. *Science* **245**, 45-48.

Biewener, A. A. (1990). Biomechanics of mammalian terrestrial locomotion. *Science* **250**, 1097-1103.

Biewener, A. A. (1991). Musculoskeletal design in relation to body size. *J. Biomech.* **24 Suppl. 1**, 19-29.

Biewener, A. A. (1992). *In vivo* measurement of bone strain and tendon force. In *Biomechanics – Structures and Systems: A Practical Approach* (ed. A. A. Biewener), pp. 123-147. New York: Oxford University Press.

Biewener, A. A. (1993). Safety factors in bone strength. *Calcif. Tissue Int.* **53 Suppl. 1**, S68-S74.

Biewener, A. A. and Dial, K. P. (1995). *In vivo* strain in the humerus of pigeons (*Columba livia*) during flight. *J. Morphol.* **225**, 61-75.

Biewener, A. A. and Taylor, C. R. (1986). Bone strain: a determinant of gait and speed? *J. Exp. Biol.* **123**, 383-400.

Biewener, A. A., Thomason, J. J., Goodship, A. and Lanyon, L. E. (1983). Bone stress in the horse forelimb during locomotion at different gaits: a comparison of two experimental methods. *J. Biomech.* **16**, 565-576.

Biewener, A. A., Swartz, S. M. and Bertram, J. E. A. (1986). Bone modeling during growth: dynamic strain equilibrium in the chick tibiotarsus. *Calcif. Tissue Int.* **39**, 390-395.

Biewener, A. A., Thomason, J. J. and Lanyon, L. E. (1988). Mechanics of locomotion and jumping in the horse (*Equus*): *in vivo* stress in the tibia and metatarsus. *J. Zool. Lond.* **214**, 547-565.

Bishop, M. J. and Friday, A. E. (1987). Tetrapod relationships: the molecular evidence. In *Molecules and Morphology in Evolution: Conflict or Compromise?* (ed. C. Patterson), pp. 123-139. Cambridge: Cambridge University Press.

Blob, R. W. (2001). Evolution of hindlimb posture in non-mammalian therapsids: biomechanical tests of paleontological hypotheses. *Paleobiology* **27**, 14-38.

Blob, R. W. and Biewener, A. A. (1999). *In vivo* locomotor strain in the hindlimb bones of *Alligator mississippiensis* and *Iguana iguana*: implications for the evolution of limb bone safety factor and non-sprawling limb posture. *J. Exp. Biol.* **202**, 1023-1046.

Blob, R. W. and Biewener, A. A. (2001). Mechanics of limb bone loading during terrestrial locomotion in the green iguana (*Iguana iguana*) and American alligator (*Alligator mississippiensis*). *J. Exp. Biol.* **204**, 1099-1122.

Blob, R. W. and Snelgrove, J. M. (2006). Antler stiffness in moose (*Alces alces*): correlated evolution of bone function and material properties? *J. Morphol.* **267**, 1075-1086.

Butcher, M. T. and Blob, R. W. (2008). Mechanics of limb bone loading during terrestrial locomotion in river cooter turtles (*Pseudemys concinna*). *J. Exp. Biol.* **211**, 1187-1202.

Butcher, M. T., Espinoza, N. R., Cirilo, S. R. and Blob, R. W. (2008). *In vivo* strains in the femur of river cooter turtles (*Pseudemys concinna*) during terrestrial locomotion: tests of force-platform models of loading mechanics. *J. Exp. Biol.* **211**, 2397-2407.

Carrano, M. T. (1998). Locomotion of non-avian dinosaurs: integrating data from hindlimb kinematics, *in vivo* strains and bone morphology. *Paleobiology* **24**, 450-469.

Carrano, M. T. and Biewener, A. A. (1999). Experimental alteration of limb posture in the chicken (*Gallus gallus*) and its bearing on the use of birds as analogs for dinosaur locomotion. *J. Morphol.* **240**, 237-249.

Carter, D. R. (1978). Anisotropic analysis of strain rosette information from cortical bone. *J. Biomech.* **11**, 199-202.

Carter, D. R., Harris, W. H., Vasu, R. and Caler, W. E. (1981). The mechanical and biological response of cortical bone to *in vivo* strain histories. In *Mechanical Properties of Bone*, Vol. 45 (ed. S. C. Cowin), pp. 81-92. New York: American Society of Mechanical Engineers.

Currey, J. D. (1984). *The Mechanical Adaptations of Bones*. Princeton, NJ: Princeton University Press.

Currey, J. D. (1990). Physical characteristics affecting the tensile failure properties of compact bone. *J. Biomech.* **23**, 837-844.

Dally, J. W. and Riley, W. F. (1978). *Experimental Strain Analysis*. New York: McGraw-Hill.

Davies, H. M. S., McCarthy, R. N. and Jeffcott, L. B. (1993). Surface strain on the dorsal metacarpus of thoroughbreds at different speeds and gaits. *Acta Anat.* **146**, 148-153.

de Ricqlès, A. J. (1975). On bone histology of living and fossil reptiles, with comments on its functional and evolutionary significance. In *Morphology and Biology of Reptiles* (ed. A. d'A. Bellairs and C. B. Cox), pp. 123-150. Linnean Society Symposium Series, Number 3. London: Academic Press.

de Ricqlès, A. J., Meunier, F. J., Castanet, J. and Francillon-Vieillot, H. (1991). Comparative microstructure of bone. In *Bone,* Vol. 3, *Bone Matrix and Bone Specific Products* (ed. B. K. Hall), pp. 1-78. Boca Raton, FL: CRC Press.

Delciellos, A. C. and Vieira, M. V. (2006). Arboreal walking performance in seven didelphid marsupials as an aspect of their fundamental niche. *Austral. Ecol.* **31**, 449-457.

Delciellos, A. C. and Vieira, M. V. (2009). Allometric, phylogenetic, and adaptive components of climbing performance in seven species of didelphid marsupials. *J. Mammal.* **90**, 104-113.

Demes, B., Qin, Y. X., Stern, J. T., Larson, S. G. and Rubin, C. T. (2001). Patterns of strain in the macaque tibia during functional activity. *Am. J. Phys. Anthropol.* **116**, 257-265.

Erickson, G. M., Catanese, J., 3rd and Keaveny, T. M. (2002). Evolution of the biomechanical material properties of the femur. *Anat. Rec.* **268**, 115-124.
Furman, B. R. and Saha, S. (2000). Torsional testing of bone. In *Mechanical Testing of Bone and the Bone-Implant Interface* (ed. Y. H. An and R. A. Draughn), pp. 219-239. Boca Raton, FL: CRC Press.
Gross, T. S., McLeod, K. J. and Rubin, C. T. (1992). Characterizing bone strain distributions *in vivo* using three rosette strain gauges. *J. Biomech.* **25**, 1081-1087.
Hopson, J. A. (1991). Systematics of the nonmammalian Synapsida and implications for patterns of evolution in synapsids. In *Origins of the Higher Groups of Tetrapods: Controversy and Consensus* (ed. H.-P. Schultze and L. Trueb), pp. 635-693. Ithaca and London: Comstock Publishing Associates.
Hopson, J. A. (1994). Synapsid evolution and the radiation of noneutherian mammals. In *Major Features of Vertebrate Evolution, Short Course in Paleontology* 7 (ed. D. R. Prothero and R. M. Schoch), pp. 190-219. Knoxville, TN: The Paleontological Society.
Jayes, A. S. and Alexander, R. McN. (1980). The gaits of chelonians: walking techniques for very slow speeds. *J. Zool. Lond.* **191**, 353-378.
Jenkins, F. A., Jr (1971a). Limb posture and locomotion in the Virginia opossum (*Didelphis marsupialis*) and in other cursorial mammals. *J. Zool. Lond.* **165**, 303-315.
Jenkins, F. A., Jr (1971b). The postcranial skeleton of African cynodonts. *Bull. Peabody Mus. Nat. Hist.* **36**, 1-216.
Jenkins, F. A., Jr and Parrington, F. R. (1976). The postcranial skeletons of the Triassic mammals *Eozostrodon, Megazostrodon* and *Erythrotherium. Philos. Trans. R. Soc. Lond. B* **273**, 387-431.
Keller, T. S. and Spengler, D. M. (1989). Regulation of bone stress and strain in the immature and mature rat femur. *J. Biomech.* **22**, 1115-1127.
Kemp, T. S. (1982). *Mammal-like Reptiles and the Origin of Mammals*. London: Academic Press.
Kemp, T. S. (1985). A functional interpretation of the transition from primitive tetrapod to mammalian locomotion. In *Principles of Construction in Fossil and Recent Reptiles* (ed. J. Reiβ and E. Frey), pp. 181-191. Stuttgart: Universität Stuttgart/ Universität Tübingen.
Kielan-Jawaroska, Z. and Gambarayan, P. P. (1994). Postcranial anatomy and habits of Asian multituberculate mammals. *Fossils Strata* **36**, 1-92.
Kirsh, J. A. W. and Mayer, G. C. (1998). The platypus is not a rodent: DNA hybridization, amniote phylogeny and the palimpsest theory. *Philos. Trans. R. Soc. Lond. B.* **353**, 1221-1237.
Lanyon, L. E. and Rubin, C. T. (1985). Functional adaptation in skeletal structures. In *Functional Vertebrate Morphology* (ed. M. Hildebrand, D. M. Bramble, K. F. Liem and D. B. Wake), pp. 1-25. Cambridge: The Belknap Press.
Lee, A. K. and Cockburn, A. (1985). *Evolutionary Ecology of Marsupials*. Cambridge: Cambridge University Press.
Lieberman, D. E., Pearson, O. M., Polk, J. D., Demes, B. and Crompton, A. W. (2003). Optimization of bone growth and remodeling in response to loading in tapered mammalian limbs. *J. Exp. Biol.* **206**, 3125-3138.
Lieberman, D. E., Polk, J. D. and Demes, B. (2004). Predicting long bone loading from cross-sectional geometry. *Am. J. Phys. Anthropol.* **123**, 156-171.
Lowell, R. B. (1985). Selection for increased safety factors of the biological structures as environmental unpredictability increases. *Science* **228**, 1009-1011.
Main, R. P. and Biewener, A. A. (2004). Ontogenetic patterns of limb loading, *in vivo* strains and growth in the goat radius. *J. Exp. Biol.* **207**, 2577-2588.
Main, R. P. and Biewener, A. A. (2007). Skeletal strain patterns and growth in the emu hindlimb during ontogeny. *J. Exp. Biol.* **210**, 2676-2690.
Meyer, A. and Zardoya, R. (2003). Recent advances in the (molecular) phylogeny of vertebrates. *Annu. Rev. Ecol. Evol. Syst.* **34**, 311-338.
Nowak, R. M. (1991). *Walker's Mammals of the World*, 5th edn. Baltimore, MD: Johns Hopkins University Press.
Peters, S. E., Mulkey, R., Rasmussen, S. A. and Goslow, G. E., Jr (1984). Motor units of the primary ankle muscles of the opossum (*Didelphis virginiana*): functional properties and fiber types. *J. Morphol.* **181**, 305-317.
Reilly, S. M. and White, T. D. (2003). Hypaxial motor patterns and the function of epipubic bones in primitive mammals. *Science* **299**, 400-402.
Reilly, S. M., Willey, J. S., Biknevicius, A. R. and Blob, R. W. (2005). Hindlimb function in the alligator: integrating movements, motor patterns, ground reaction forces and bone strain of terrestrial locomotion. *J. Exp. Biol.* **208**, 993-1009.
Romer, A. S. (1922). The locomotor apparatus of certain primitive and mammal-like reptiles. *Bull. Am. Mus. Nat. Hist.* **46**, 517-606.
Rubin, C. T. and Lanyon, L. E. (1982). Limb mechanics as a function of speed and gait: a study of functional strains in the radius and tibia of horse and dog. *J. Exp. Biol.* **101**, 187-211.
Sheffield, K. M. and Blob, R. W. (2011). Loading mechanics of the femur in tiger salamanders (*Ambystoma tigrinum*) during terrestrial locomotion. *J. Exp. Biol.* **214**, 2603-2615.
Sheffield, K. M., Butcher, M. T., Shugart, S. K., Gander, J. C. and Blob, R. W. Locomotor loading mechanics in the hindlimbs of tegu lizards (*Tupinambis merianae)*: comparative and evolutionary implications. *J. Exp. Biol.* **214**, 2616-2630.
Szivek, J. A., Johnson, E. M. and Magee, F. P. (1992). *In vivo* strain analysis of the greyhound femoral diaphysis. *J. Invest. Surg.* **5**, 91-108.
Voss, R. S. and Jansa, S. A. (2009). Phylogenetic relationships and classification of didelphid marsupials, an extant radiation of New World metatherian mammals. *Bull. Am. Mus. Nat. Hist.* **322**, 1-177.
White, T. D. (1990). Gait selection in the brush-tail possum (*Trichosurus vulpecula*), the northern quoll (*Dasyurus hallucatus*), and the Virginia opossum (*Didelphis virginiana*). *J. Mammol.* **71**, 79-84.
Wilson, M. P., Espinoza, N. R., Shah, S. R. and Blob, R. W. (2009). Mechanical properties of the hindlimb bones of bullfrogs and cane toads in bending and torsion. *Anat. Rec.* **292**, 935-944.